IIETA International Information and Engineering Technology Association
Advancing the World of Information and Engineering

INTERNATIONAL JOURNAL OF HEAT AND TECHNOLOGY
Vol.33, No.1, 2015

CFD INVESTIGATION OF VORTEX TUBE LENGTH EFFECT AS A DESIGNING CRITERION

Nader Pourmahmoud*, Reza Esmaily°, Amir Hassanzadeh °**

* Mechanical Engineering Department, Urmia University, Urmia, Iran;
° Sama Technical and Vocational Training College, I.A.U., Mahabad Branch, Mahabad, Iran

ABSTRACT

In this article a computational fluid dynamics model is used to simulate the flow field structure in the machine, in order to study the effects of various parameters on the performance and temperature separation. The investigations have been carried out to realize the effect of length and other parameters such as inlet pressure and nozzles on the behavior of vortex tube. Attention has been focused on the stagnation point and the performance of a vortex tube as a simple device, operating as a refrigerating machine having no moving parts. The CFD model has involved a turbulent, compressible and axisymmetric swirling flow that utilizes the standard k-ε turbulence model. The numerically simulated vortex tube has two straight nozzles with axial outlet streams. The performance curves of numerical evaluations such as temperature separation versus cold mass fraction were obtained for a specific vortex tube with a given inlet thermo physical properties. Numerical results are obtained for various amounts of cold mass fractions. Therefore, geometrical study of mechanical components such as tube length, nozzles numbers, stagnation point, wall temperature and also inlet gas pressure effects on the machine operation have been presented in the more details as the research main goals.

KEYWORDS: Ranque-Hilsch vortex tube, CFD simulation, Stagnation point, Energy separation, Inlet Pressure.

1. INTRODUCTION

Vortex tube or Ranque-Hilsch vortex tube is a mechanical device with a simple geometry, which is able to conforms the entrance tangential air into to different hot and cold division. The compressed air enters the tube tangentially through one or more nozzles. This instrument doesn't have any mobile part and divides the air into two different hot and cold current without any working fluid or electrical energy. They each can be used according to the basic requirement. However the essential function of vortex tube is in cooling. The main fluid in vortex tube is air. Figure 1. This device was invented many years ago, when the first time it was discovered accidentally by a French physicist named George Ranque in 1931 [1] while was conducting a research over vortex tube in the field of dust separation. He noticed the emitting of hot air from onside and cold air from another side. A few years later, in 1945 German physicist (Rudolf Hilsch) worked on vortex tube consequently. He developed the vortex tube and worked on its design. He finally published the results of his works in an article in 1947 [2]. Figure 1 shows a schematic diagram of a vortex tube and its flow patterns.

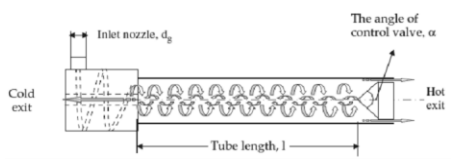

Figure 1. Schematic drawing of a vortex tube and its components

In recent years, the techniques of computational fluid dynamics (CFD) modeling have been developed for more survey and clarification. Harnett and Eckert [3] invoked turbulent eddies, Ahlborn and Gordon, [4] described an embedded secondary circulation and Stephan et al. [5] proposed the formation of Gortler vortices on the inside wall of the vortex tube that drive the fluid motion. Kurosaka [6] reported the temperature separation to be a result of acoustic streaming effect that transfers energy from the cold core to the hot outer annulus. Aljuwayhel et al. [7] utilized a fluid dynamics model of the vortex tube to understand the process that drives the temperature separation phenomena. Skye et al. [8] used a model similar to that of Aljuwayhel et al. [7]. Chang et al. [9] conducted a visualization experiment using surface tracing method to investigation the internal flow phenomena and to indicate the stagnation position in a vortex tube. Eisma and Promvonge. [10] performed a numerical study to research the flow field and temperature separation phenomenon.

Pourmahmoud et al. [11] investigated numerically the effect of inlet pressure importance in flow patterns. Also Pourmahmoud et al. [12] studied numerically the effect of helical nozzles on the energy separation in a vortex tube. They concluded that this type of nozzles increase the swirl velocity as well as cold exit temperature difference. Kirmaci [13] used Taguchi method to optimize the number of nozzle of vortex tube. While each of these explanations may capture certain aspects of vortex tube, none of these mechanisms altogether explains the vortex tube effect. Vortex tubes

generally are used as a cooling system for Industrial purposes. Pourmahmoud et al. [25] studied the effect of convergent nozzles on the energy separation in a vortex tube.

Rafiee et al. [26] investigated the radius of working tube numerically. Among analytical works done on the vortex tube; Lorenzini and Spiga [27] studied the flow field inside vortex tube. They drived relations for velocity components inside vortex tube.

2. NUMERICAL MODELING AND GOVERNING EQUATIONS

The numerical simulation of the vortex tube has been created by using the FLUENTTM software package. The models are three dimensional, steady state and compressible and employ the standard k-epsilon turbulence model [14]. The compressible turbulent flows in the vortex tube are governed by the conservation of mass, momentum and energy equations. The mass and momentum conservation and the state equation are solved as follows:

$$\frac{\partial}{\partial x_j}(\rho u_j) = 0 \tag{1}$$

$$\frac{\partial}{\partial x_j}(\rho u_i u_j) = -\frac{\partial p}{\partial x_i} + \frac{\partial}{\partial x_j}\left[\mu\left(\frac{\partial u_i}{\partial x_j} + \frac{\partial u_j}{\partial x_i} - \frac{2}{3}\delta_{ij}\frac{\partial u_k}{\partial x_k}\right)\right] + \frac{\partial}{\partial x_j}(-\overline{\rho u_i' u_j'}) \tag{2}$$

$$\frac{\partial}{\partial x_i}\left[u_i \rho\left(h + \frac{1}{2}u_j u_j\right)\right] = \frac{\partial}{\partial x_j}\left[k_{eff}\frac{\partial T}{\partial x_j} + u_i(\tau_{ij})_{eff}\right] \tag{3}$$

$$k_{eff} = K + \frac{c_p \mu_t}{\mathrm{Pr}_t}$$

and

The state equation is necessary for an ideal gas, because of compressibility effect and given as:

$$p = \rho R T \tag{4}$$

The flow field throughout the vortex tube is fully turbulent. Thus, the turbulence kinetic energy, k, and its rate of dissipation, ε, are obtained from the following transport equations:

$$\frac{\partial}{\partial t}(\rho k) + \frac{\partial}{\partial x_i}(\rho k u_i) = \frac{\partial}{\partial x_j}[(\mu + \frac{\mu_t}{\sigma_k})\frac{\partial k}{\partial x_j}] + G_k + G_b - \rho\varepsilon - Y_M \tag{5}$$

$$\frac{\partial}{\partial t}(\rho k) + \frac{\partial}{\partial x_i}(\rho k u_i) = \frac{\partial}{\partial x_j}[(\mu + \frac{\mu_t}{\sigma_\varepsilon})\frac{\partial \varepsilon}{\partial x_j}] + C_{1\varepsilon}\frac{\varepsilon}{k}(G_k + C_{3\varepsilon}G_b) - C_{2\varepsilon}\rho\frac{\varepsilon^2}{k} \tag{6}$$

where, G_k represents the generation of turbulence kinetic energy due to the mean velocity gradients and G_b is the generation of turbulence kinetic energy due to buoyancy which is neglected in this case. Y_M represents the contribution of the fluctuating in compressible turbulence to the overall dissipation rate and $C_{1\varepsilon}$, $C_{2\varepsilon}$ and $C_{3\varepsilon}$ are coefficients. σ_k and σ_ε are the turbulent prandtl numbers for k and ε, respectively.

The turbulent viscosity, μ_t , is computed by combining k and ε as follows:

$$\mu_t = \rho C_\mu \frac{k^2}{\varepsilon} \tag{7}$$

Where, C_μ is a constant. The model constants $C_{1\varepsilon}$, $C_{2\varepsilon}$, C_μ, σ_k and σ_ε have the following default values: $C_{1\varepsilon}$ = 1.44, $C_{2\varepsilon}$ = 1.92, C_μ = 0.09, σ_k = 1.0, σ_ε = 1.3.

An important parameter in the vortex tube study is α which is defined as cold mass fraction parameter. Its conventional definition is:

$$\alpha = \frac{\dot{m}_c}{\dot{m}_{in}} \tag{8}$$

Where $\dot{m}_c$ is cold mass flow rate and $\dot{m}_{in}$ is inlet mass flow rate. The cold exit temperature difference ($\Delta T_{i,c}$) and the hot exit temperature difference ($\Delta T_{h,i}$) and the total temperature difference (ΔT) of the vortex tube are defined as following, respectively:

$$\Delta T_{i,c} = T_i - T_c \tag{9}$$

$$\Delta T_{i,h} = T_h - T_i \tag{10}$$

$$\Delta T = T_h - T_c \tag{11}$$

Boundary conditions for the models are determined as following: The inlet is modeled as a pressure inlet. The static pressure at the cold exit boundary was fixed at 0.15 bar. The static pressure at the hot exit boundary is adjusted in the way to vary the cold mass fraction. The second-order numerical schemes were used to discretize derivatives terms of governing equations during the computational procedure.

3. PHYSICAL MODELING

To study the effect of length on the performance of vortex tube, all geometrical properties of the CFD models are kept constant. By varying the length of the model, eight models with different lengths and two numbers of straight nozzles were created. The radius of the vortex tubes fixed at 4.5 mm, and the length are set to 82, 87, 90, 92, 94, 98, 100 and 105 mm, respectively. The geometry summary is given in tab. 1. Since the nozzle consists of 2 straight slots, the CFD model has been assumed to be a rotational periodic flow and only a sector of the flow domain with angle of 180°. The three-dimension CFD model with refinement in mesh along with boundary regions is shown in Fig. 2.

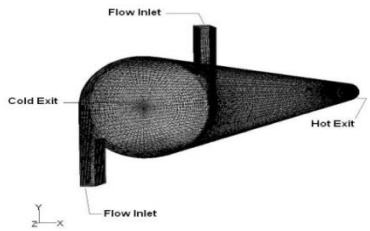

Figure 2. Three-dimensional CFD model of vortex tube with two straight nozzles

Table 1. Geometry summary of the CFD model of vortex tube

Measurement	Value
Working tube length	Varied
Vortex tube Diameter	8.5 mm
Nozzle height	2 mm
Nozzle width	1 mm
Nozzle total inlet area (An)	4 mm^2
Cold exit diameter	4 mm
Cold exit area	12.6 mm^2
Hot exit thickness	8 mm
Hot exit area	6.48 mm^2

4. GRID INDEPENDENCE STUDY

To remove the errors due to coarseness of grid, analysis has been carried out for different average unit cell volumes in a vortex tube with length of 90 mm and cold mass fraction equals 0.2. The variation of cold exit temperature difference as key parameter is shown in Fig. 3, for different unit cell volumes. It can be seen that not much advantage in reducing the unit cell volume size below 0.0356 mm^3 which corresponds to 400000 cells for the configuration studied.

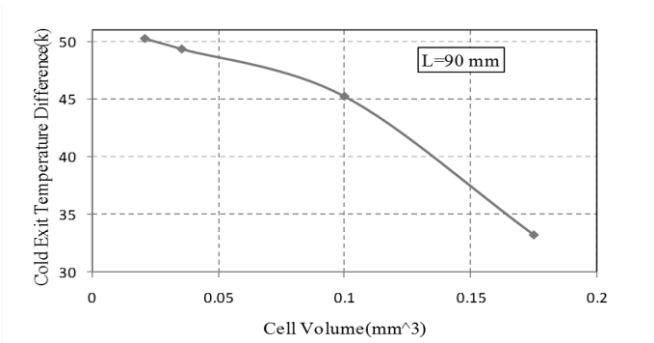

Figure 3. Grid independency for vortex tube with 92 mm length and P=7 bar

5. INVESTIGATION OF LENGTH EFFECT

Many experimental and numerical investigations have been done on length to diameter ratio so far such as [2, 15-17]. However the effect of length on the location of stagnation point has been less investigated. It can be mentioned to Bramo and Pourmahmoud [18] that studied the operation of vortex tube with different length to diameter ratios and investigated the location of stagnation point on the temperature difference.

The stagnation point position within the vortex tube can be established from the velocity profile along the tube length at the point where axial velocity ceases to have a negative value. Figure 4 shows the stagnation point and streamlines in the r–z plane associated with the flow inside the optimum vortex tube.

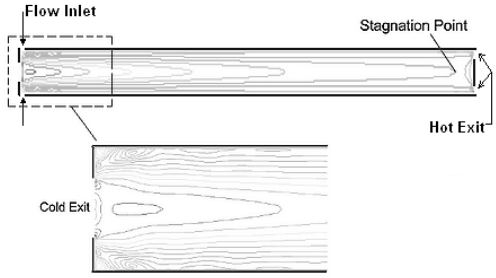

Figure 4. Streamlines of vortex tube in r–z plane.

In the present research, vortex tube with different lengths of 82, 87, 90, 92, 94, 98, 100 and 105 mm are investigated numerically. The inlet pressure is 7 bar. Figure 5 displays the axial velocity in centerline of tube for all models. As seen for $L \leq 94$ mm the location of stagnation point doest change and is located in nearest position to hot exit. By increasing the length up to 94 mm, the location of stagnation point changes suddenly and it comes into the cold exit. This causes to decrease the cold temperature difference.

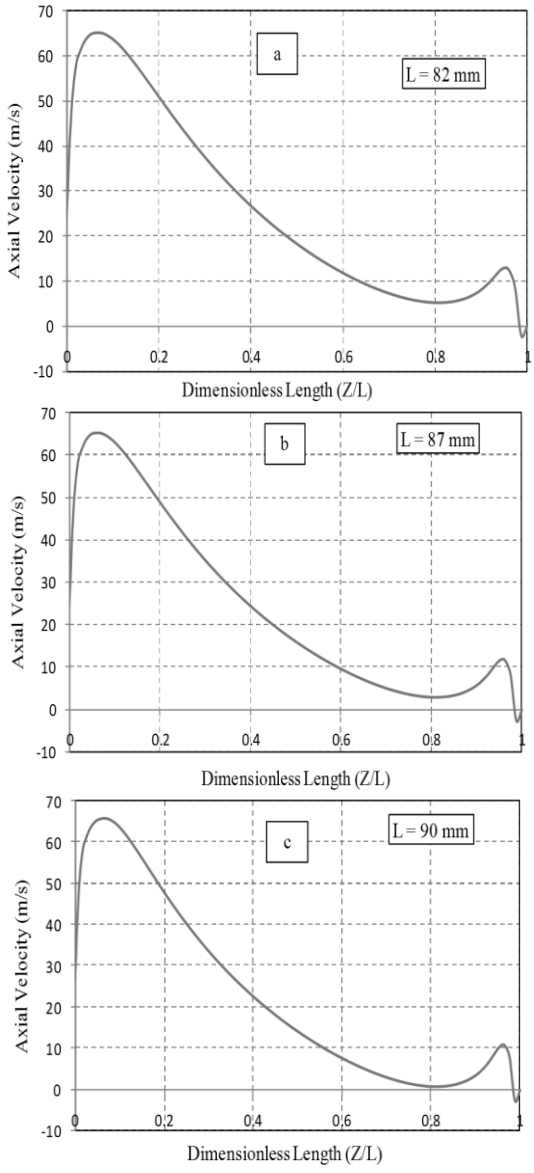

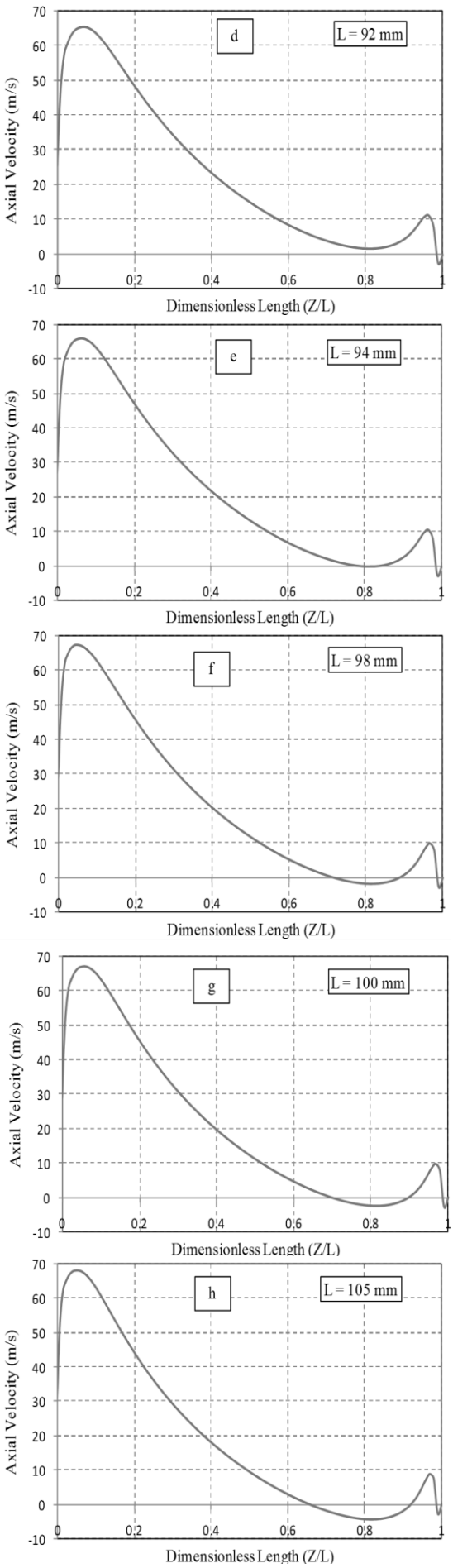

Figure 5. Variation of axial velocity along the center line of the vortex tube

The summary of stagnation point location for different lengths is displayed in Fig. 6 and the maximum cold temperature difference produced by CFD models is displayed in Fig. 7 for mass fraction of 0.2. It can be seen that vortex tube with length of 90 mm has maximum cold temperature difference equals to 49.295 K. Figure 8 displays hot temperature difference for CFD models. The hot temperature difference increases by increasing of length. Moreover the purpose of this article is to design of vortex tube with maximum hot temperature difference the paper does not focus on this parameter. From results of this section it can be concluded that vortex tube with length of 90 mm produces maximum cold difference. Therefore it can be chosen as optimum vortex tube and further investigations will be held on it.

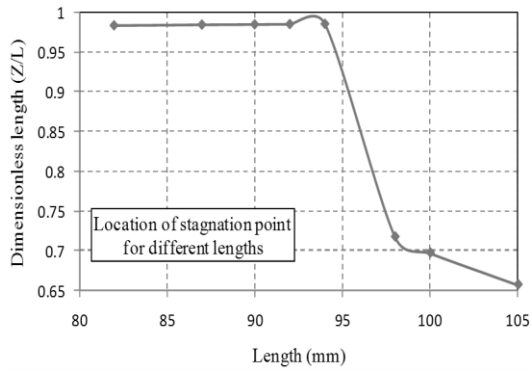

Figure 6. Location of stagnation point occurred in vortex tube with different lengths

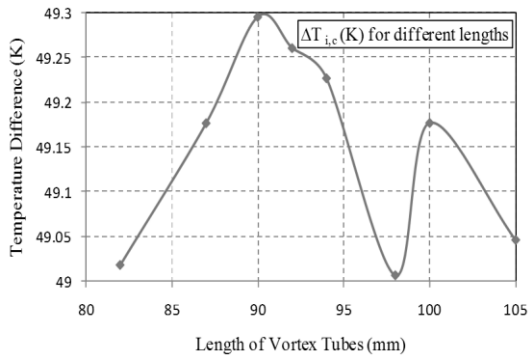

Figure 7. Maximum cold exit temperature difference obtained at different lengths

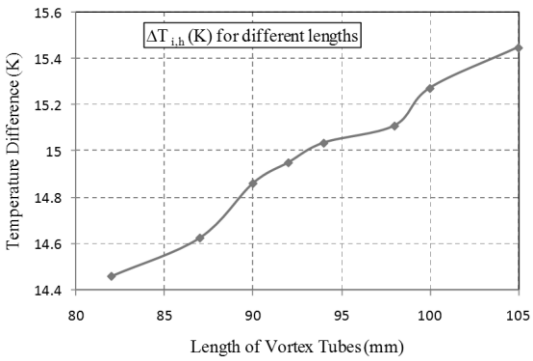

Figure 8. Maximum hot exit temperature difference obtained at different lengths

Figure 9 shows the temperature counters distribution in a longitudinal cross section of tube, when cold mass fraction is varied. These results help to realize the formation and configuration of fluid layers temperature in the both axial and radial directions in the tube. It is seen that, for temperature contours in Fig. 9 temperature gradients are high in the region near the tube wall and are small in the core region. It is of interest to note that the entire flow, except for the outer annular ring, is at a total temperature lower than the inlet temperature, Tin. The separation of the total temperature field into regions of high energy (high total temperature) along the tube wall and low energy is evident in Fig. 9 which shows that the total temperature is a minimum in the central region. The separation effect or temperature difference for the total temperature is large near the core of the inlet region and decreases as the exit is approached.

Figure 9. Temperature distribution counters for L = 92 mm

6. INLET PRESSURE AND WALL TEMPERATURE EFFECT

In this section the optimized model with length of 90 mm is investigated numerically. For this purpose the model is tested for 5, 6 and 7 bar pressure. Fig. 10 displays temperature difference between cold exit and inlet ($\Delta T_{i,c}$ (K)) for different cold mass fractions. As shown in a constant cold mass fraction, cold temperature difference increases by increasing the pressure. Moreover, in a constant pressure, cold temperature difference decreases by increasing the cold mass fraction. The maximum cold temperature difference is for cold mass fraction of 0.2 in each pressure. Figure 11 displays temperature difference between hot exit and inlet ($\Delta T_{i,h}$ (K)) for different cold mass fractions. As shown in a constant cold mass fraction, hot temperature difference increases by increasing the pressure. However this increase is low. Moreover, in a constant pressure, hot temperature difference increases by increasing the cold mass fraction. The maximum hot temperature difference is for cold mass fraction of 0.8 in each pressure.

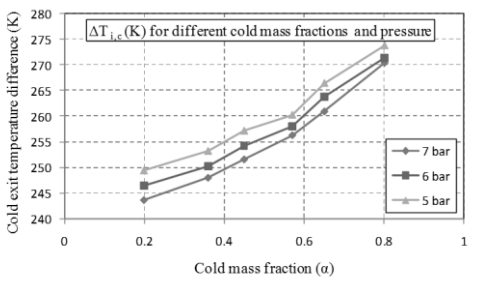

Figure 10. $\Delta T_{i,c}$ for different inlet pressures

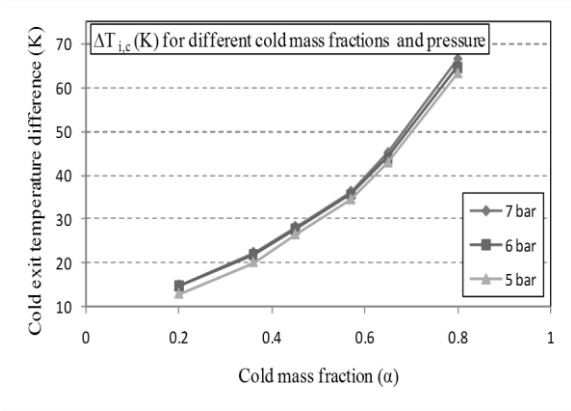

Figure 11. Hot exit temperature difference for different inlet pressures

From these results, it can be found that pressure is the most effective parameter in cooling and heating operating of vortex tube. If the inlet pressure increases the amount of temperature difference for both cold and hot exits increase too. Because in the vortex chamber, the air which is nearer to the wall will be compressed and air in the center region will be expanded. Hence, the outer core will be heated and the inner core will be cooled [19]. The other reason is due to the fact that at high pressure, air enters the vortex tube with a higher tangential velocity, resulting in higher momentum transfer from the central region of the tube to the tube wall [20].

The results of present study show that the performance of vortex tubes can be related to position of stagnation point along tube length. The axial position of this point is precisely determined from the velocity profile along the tube length, where axial velocity ceases to have a negative value. Also, it can be explored according to location of maximum wall temperature, where it reaches to a maximum value. Physical mechanism of energy separation in vortex tube would be related to exist of two counter flows in the tube because of stagnation point presence, although these two locations are not exactly coincide to each other. The stagnation point position within the vortex tube can be determined by two ways: according to maximum wall temperature location, and on the basis of velocity profile along the tube length at the point where it ceases to a negative value. The point of maximum wall temperature represents the stagnation point determined by Fulton [21]. It was assumed that the wall temperature is almost equal to gas temperature that was reported by Frohlingsdorf and Unger [22]. The numerical results suggested that considerable or the most part of energy separation in the vortex tube occurs before stagnation point. Beside to attain maximum swirl velocity and maximum cold temperature difference, axial velocity distribution together with maximum wall temperature location also would be another two important parameters in designing of a good vortex tube.

Thus, in the present investigation the wall temperature has been measured numerically along the tube length in different positions as shown in Fig. 12 for P = 5, 6 and 7 bar and cold mass fraction is fixed to 0.2. The Z/L represents a dimensionless length of vortex tube. As indicated in Fig. 13, there is an axial distance between cold and hot ends that the velocity magnitude comes to zero, and this point is specified as the stagnation point position. The results show that the positions of stagnation points for all of models are too close

to the hot exit. But, 7 bar inlet pressure causes the position of this point is drawn rather a little to the hot exit end. The axial locations of these pointes relative to hot exit end can be arranged as: first for 7 bar, second 6 bar and finally 5 bar, respectively. One can consider due to somewhat closeness of separation point of 7 bar to the hot exit, it brings maximum cold temperature difference in this type of vortex tube. As a rough estimation, according to figure 13, these arrangements lead to achieve greater wall temperature of 7 bar and then 6 bar relative to 5 bar.

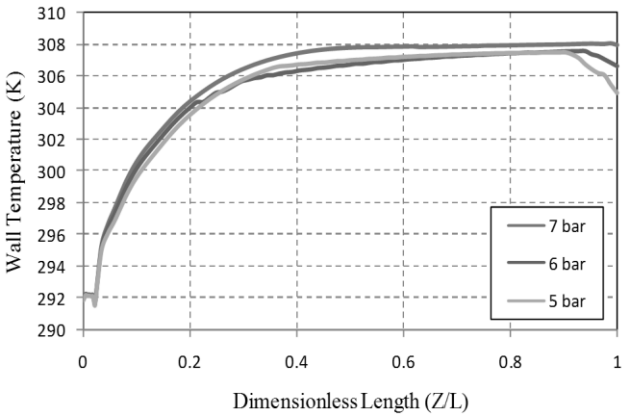

Figure 12. The variations of wall temperature along the vortex tube length of 92 mm and different pressure

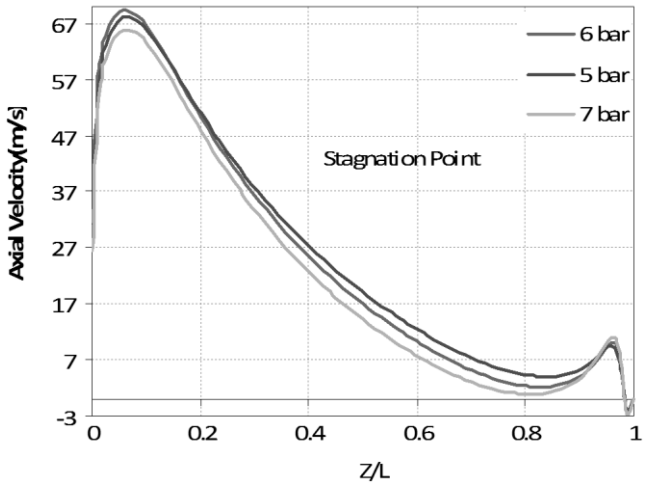

Figure 13. Axial velocity in centerline of vortex tube with length of 92 mm and different pressure

7. INFLUENCE OF NUMBER OF NOZZELS

On basis of the conclusions for straight nozzles, some reported that increasing the number of nozzles can produce a strong swirling flow field inside the vortex tube and consequently help to improve the temperature separation procedure whereas, some researchers (Yilmaz et al., [23]) said that the vortex tubes performance decreases with the increase of the nozzles number due to the development of the turbulent flow filed. To clarify the inlet nozzles number effect on the performance of vortex tube, three different CFD set of convergent nozzles, 2, 3, and 6, were designed numerically. In all cases the inlet cross-sectional area of nozzles is kept constant. Variation of the cold and hot exit gases temperature versus the cold mass fraction ratio are illustrated in Fig. 14 and 15.

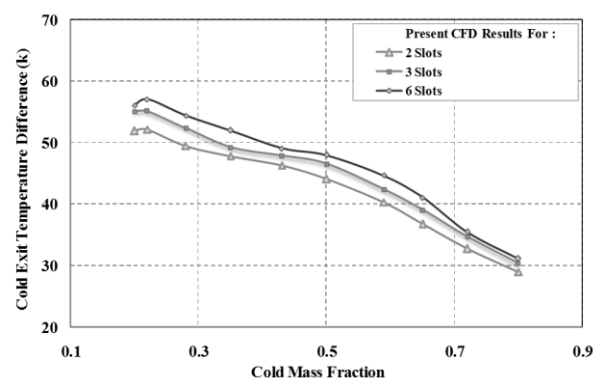

Figure 14. Effect of number of nozzle on the cold exit temperature difference: L=92 mm and P = 7 bar

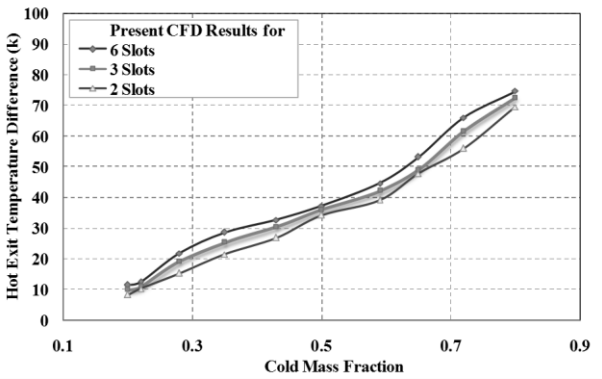

Figure 15. Effect of number of nozzle on the hot exit temperature difference: L=92 mm and P = 7 bar

As the number of nozzles increase, significantly momentum is injected to the flow field in the vortex chamber. Therefore, each nozzle plays a considerable role in pushing of adjusting flow mass toward the next nozzle. Then, the energy and temperature separation, and consequently cold temperature difference increases. In summary, it must be mentioned that the vortex tube with six intakes, as a refrigeration devise, shows better performance than two and three intake nozzles set. Furthermore, the importance of having higher peripheral velocity in the portion of vortex chamber to achieve the best energy separation is emphasized again in this machine. The velocity vectors are shown in Fig. 16 through present numerical modeling of each of three nozzles set. Results of this figure clearly illustrate that the peripheral velocity in the portion of the tube immediately after the nozzles increases, while the number of inlet nozzles increase. Hence, increasing of nozzles number, given rise to swirl velocity in the vortex chamber that is a capability enhancement in energy separation. Of course, existence of logical correlation between the swirl velocity and specially cold temperature difference has been demonstrated in all of previous researches of vortex tube ([24]).

The economic power consumption to supply high pressure gas for operating of vortex tube is important as well as our goal of producing maximum cold exit temperature difference. Vortex tube with 6 nozzles, apparently produces maximum cold temperature difference, however it should be regarded that power consumption also is intensively increased. Hence,

it is recommended to use of the vortex tube with 2 or maximum 3 number of nozzles, while the cold mass fraction in all cases must be fixed to 0.2.

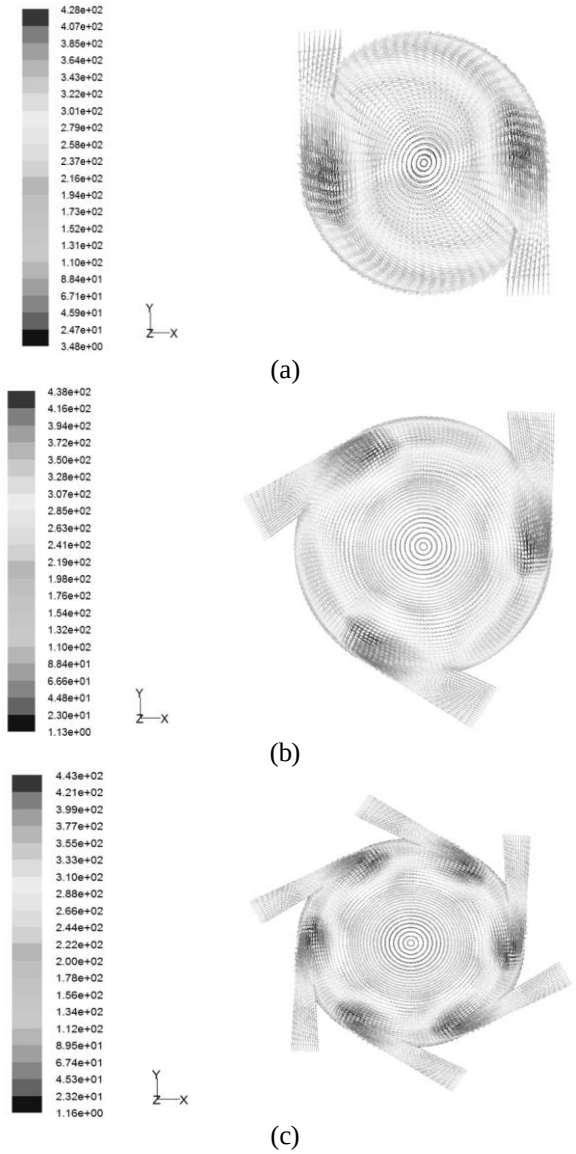

Figure 16. Velocity vectors at the vortex chamber (a) Two nozzles set(b) Three nozzles set (c) Six nozzles set

8. CONCLUSION

A numerical study has been carried out to simulate a three dimensional, compressible, and turbulent fluid flow throughout a vortex tube. In this research it has been assumed an axisymmetric geometry and steady state flow, and for exhibiting of turbulent flow structure inside vortex tube the standard k-ε turbulence model is employed. Simulations were conducted at many different tube lengths, nozzles number and cold mass fractions by changing the hot exit area. The effects of inlet pressure, tube length, nozzle number, stagnation point, wall temperature and cold mass fraction on the temperature separation were studied and lead to attain a reasonable dimensional geometry of vortex tube just on these principles. The cold mass fraction was also varied by means of changing hot exit area. So that, a vortex tube with length 92 mm and effective cold mass fraction 0.2 gives the best performance for designed machine from cooling point of view. Study of parameters such as stagnation point axial location on the tube centerline and its correlation with maximum wall temperature position revealed a reasonable agreement. The influence of inlet nozzle number is also very evident, because its increase improves the performance of the vortex tube. The measured results with different cold mass fractions suggest that small amount of this parameter gives best results in cold exit temperature difference. In addition, the tube length L, the geometry of the nozzle (type and sizes) and the cold mass fraction are important parameters in operating of vortex tube.

REFERENCES

1. G.J. Ranque, Experiments on expansion in a vortex with simultaneous exhaust of hot air and cold air, *J. Phys. Radium (Paris)*, vol. 4, pp. 112-115, 1933.
2. R. Hilsch, The use of expansion of gases in a centrifugal field as a cooling process, *Rev. Sci. Instrum*, vol. 18, pp. 108-113, 1947.
3. J. Harnett and E. Eckert, Experimental study of the velocity and temperature distribution in a high velocity vortex-type flow, *Trans. ASME* , vol.79, pp. 751-758, 1957.
4. B.K. Ahlborn and J.M. Gordon, The vortex tube as a classic thermodynamic refrigeration cycle, *J. Appl. Phys*, vol. 88 (6), pp. 3645-3653, 2000.
5. K. Stephan, S. Lin, M. Durst, F. Huang and D. Seher, An investigation of energy separation in a vortex tube, *Int. J. Heat Mass Transfer*, vol. 26 (3), pp. 341–348, 1983.
6. M. Kurosaka, Acoustic streaming in swirling flows, *J. Fluid Mech*, vol. 124, pp. 139-172, 1982.
7. N.F. Aljuwayhel, G.F. Nellis, S.A. Klein, Parametric and internal study of the vortex tube using a CFD model, *Int. J. Refrigeration*, vol. 28, pp. 442-450, 2005.
8. H.M. Skye, G.F. Nellis, S.A. Klein, Comparison of CFD analysis to empirical data in a commercial vortex tube, *Int. J. Refrigeration*, vol. 29, pp. 71-80, 2006.
9. H.S. Chang, Experimental and numerical studies in a vortex tube, *J. Mech. Sci. Tech*., vol. 20 (3), pp. 418-425, 2006.
10. S. Eisma-ard, and S. Promvonge, Numerical investigations of the thermal separation in a Ranque-Hilsch vortex tube, *Int. J. Heat Mass Transfer*, vol. 50, pp. 821-32, 2007.
11. N. Pourmahmoud, A. Hassanzadeh and O. Moutaby, Numerical investigation of operating pressure effects on the performance of a vortex tube, *Therm. Sci.*, vol. 18(2), pp. 507-520, 2014.
12. N. Pourmahmoud, A. Hassanzadeh and O. Moutaby, Numerical analysis of the effect of helical nozzles gap on the cooling capacity of Ranque–Hilsch vortex tube, *Int. J. Refrigeration*, vol. 35(5), pp. 1473-1483, 2012.
13. V. Kirmaci, Optimization of counter flow Ranque-Hilsch vortex tube performance using Taguchi method, *Int. J. Refrigeration*, vol. 32, pp. 1487-1494, 2009.
14. S. Akhesmeh, N. Pourmahmoud and H. Sedgi, Numerical study of the temperature separation in the Ranque-Hilsch vortex tube, *Am. J. Eng. Appl. Sci*, vol. 3, pp. 181-187, 2008.
15. P.K. Singh, R.G. Tathgir, D. Gangacharyulu and G.S. Grewal, An Experimental Performance Evaluation of Vortex Tube, *IE (I) Journal.MC*, vol. 84, pp. 149-153, 2004.

16. O. Aydin and M. Baki, An experimental study on the design parameters of a counter flow vortex tube, *Energy*, vol. 31(14), pp. 2763-2772, 2006.
17. K. Dincer, S. Tasdemir, S. Baskaya and B.Z. Uysal, Modeling of the effects of length to diameter ratio and nozzle number on the performance of counter flow Ranque-Hilsch vortex tubes using artificial neural networks, *App. Therm. Eng.*, vol. 28, pp. 2380-2390, 2008.
18. A.R. Bramo and N. Pourmahmoud, CFD simulation of length to diameter ratio effect on the energy separation in a vortex tube, *Therm. Sci*., vol. 15(3), pp. 833-848, 2011.
19. J. Prabakaran and S. Vaidyanathan, Effect of diameter of orifice and nozzle on the performance of counter flow vortex tube, *Int. J. Eng. Sci. Tech.*, vol. 2(4), pp. 704-707, 2010.
20. S. Eiamsa-ard, Experimental investigation of energy separation in a counter-flow Ranque–Hilsch vortex tube with multiple inlet snail entries, *Int. Comm. Heat Mass Transfer*, vol. 37, pp. 637–643, 2010.
21. C.D. Fulton, Ranque's tube, *J. Refrigeration Eng.*, vol. 5, pp. 473–479, 1950.
22. W. Frohlingsdorf and H. Unger, Numerical investigations of the compressible flow and the energy separation in the Ranque-Hilsch vortex tube, *Int. J. Heat Mass Transfer*, vol. 42, pp. 415-422, 1999.
23. M. Yilmaz, M. Kaya, S. Karagoz and S. Erdogan, A review on design criteria for vortex tubes, *Heat Mass Transfer*, vol. 45, pp. 613-632, 2009.
24. N. Pourmahmoud, A. Hassanzadeh, O. Moutaby and A.R. Bramo, Computational fluid dynamics analysis of helical nozzles effects on the energy separation in a vortex tube. *Therm. Sci*., vol. 16(1), pp. 151–166, 2012.
25. N. Pourmahmoud, A. Hassanzadeh, E. Rafiee and M. Rahimi, Three-Dimensional numerical investigation of effect of convergent nozzles on the energy separation in a vortex tube, *Int. J. Heat Tech.*, vol. 30(2), pp. 133-140, 2012.
26. S. E. Rafiee, M. Rahimi and N. Pourmahmoud, Three-Dimensional numerical investigation on a commercial vortex tube based on an experimental model - Part I: Optimaztion of the working tube radius, *Int. J. Heat Tech.*, vol. 31(1), pp. 49-56, 2013.
27. E. Lorenzini and M. Spiga, Fluid dynamic isotopic separation by the Hilsch vortex tube (in Italian), *Ingegneria*, n. 5-6, pp. 121-126, Maggio-Giugno, 1982.

NOMENCLATURE

D	Diameter of vortex tube [mm]
k	Turbulence kinetic energy [$m^2 s^{-2}$]
L	Length of vortex tube [mm]
P	Pressure [Pa]
r	Radial distance measured from the centerline of tube [mm]
R	Radius of vortex tube
T	Temperature [K]
z	Axial length from nozzle cross section [mm]

GREEK SYMBOLS

	Cold mass fraction
β	Convergence angle of nozzles
	Turbulence dissipation rate [$m^2 s^{-3}$]
$_{i,c}$	Temperature difference between inlet and cold ends [K]
$_{i,h}$	Temperature difference between hot end and inlet [K]
	Density [$kg\ m^{-3}$]
	Dynamic viscosity [$kg\ m^{-1} s^{-1}$]
$_t$	Turbulent viscosity [$kg\ m^{-1} s^{-1}$]
$_{ij}$	Stress tensor components

SUBSCRIPTS

c	Cold
h	Hot
i	Inlet